

Aqueous Photochemistry of Secondary Organic Aerosol of α -Pinene and α -Humulene Oxidized with Ozone, Hydroxyl Radical, and Nitrate Radical

Dian E. Romonosky,[†] Ying Li,[‡] Manabu Shiraiwa,[†] Alexander Laskin,[§] Julia Laskin,^{||} and Sergey A. Nizkorodov^{*,†}

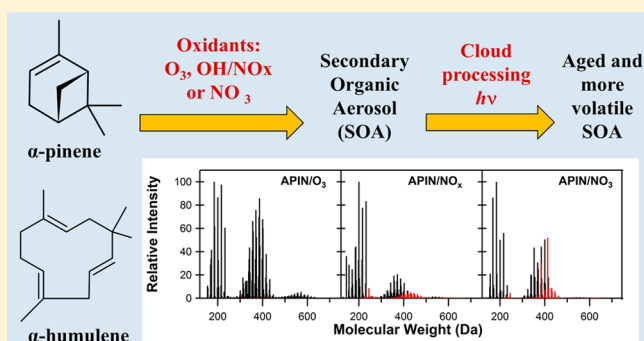
[†]Department of Chemistry, University of California, Irvine, California 92697, United States

[‡]National Institute for Environmental Studies, Tsukuba, Ibaraki 305-8506, Japan

[§]Environmental Molecular Sciences Laboratory and ^{||}Physical Sciences Division, Pacific Northwest National Laboratory, Richland, Washington 99352, United States

Supporting Information

ABSTRACT: Formation of secondary organic aerosols (SOA) from biogenic volatile organic compounds (BVOC) occurs via O_3 - and OH-initiated reactions during the day and reactions with NO_3 during the night. We explored the effect of these three oxidation conditions on the molecular composition and aqueous photochemistry of model SOA prepared from two common BVOC. A common monoterpene, α -pinene, and sesquiterpene, α -humulene, were used to form SOA in a smog chamber via $BVOC + O_3$, $BVOC + NO_3$, and $BVOC + OH + NO_x$ oxidation. Samples of SOA were collected on filters, water-soluble compounds from SOA were extracted in water, and the resulting aqueous solutions were photolyzed to simulate the photochemical aqueous processing of SOA. The extent of change in the molecular level composition of SOA over 4 h of photolysis (approximately equivalent to 64 h of photolysis under ambient conditions) was assessed with high-resolution electrospray ionization mass spectrometry. The analysis revealed significant differences in the molecular composition between SOA formed by the different oxidation pathways. The composition further evolved during photolysis with the most notable change corresponding to the nearly complete removal of nitrogen-containing organic compounds. Hydrolysis of SOA compounds also occurred in parallel with photolysis. The preferential loss of larger SOA compounds during photolysis and hydrolysis made the SOA compounds more volatile on average. This study suggests that aqueous processes may under certain conditions lead to a reduction in the SOA loading as opposed to an increase in SOA loading commonly assumed in the literature.



INTRODUCTION

Secondary organic aerosols (SOA) produced by the gas- and aqueous-phase oxidation of biogenic volatile organic compounds (BVOC) have both health and climate relevance.¹ Following the initial formation, SOA are known to undergo chemical aging processes from reactions with sunlight and atmospheric oxidants.^{2,3} The mechanisms of chemical aging and the role of aging processes in determining climate and health relevant properties of SOA, such as saturation vapor pressures of the SOA compounds, remain poorly explored.⁴ Part of the challenge is the inherent chemical complexity of both SOA and their aging processes.⁵

Aqueous processing of atmospheric organic compounds include reactions with aqueous oxidants and aqueous photolysis and is now recognized as an important mechanism of chemical aging of SOA.^{6,7} The SOA particles produced from BVOC often nucleate cloud and fog droplets making the SOA compounds dissolved and accessible to the aqueous photo-

chemical processes. We previously showed that exposure of dissolved SOA produced from a number of VOC precursors to actinic radiation leads to significant changes in the molecular composition of SOA.^{8–10} The effect of photolysis on SOA composition was greater for SOA prepared by ozonolysis of VOC in dark conditions compared to that for SOA prepared by OH + NO_x photooxidation of VOC.¹⁰ This is a reasonable result as the most photolabile compounds are photolyzed already during the photooxidation in the smog chamber. Formation of SOA in the $BVOC + NO_3$ reactions is another example of a process that occurs in dark conditions. This type of SOA may contain a larger fraction of photolabile molecules relative to the SOA prepared from the same VOC under OH + NO_x photooxidation conditions. If this were correct, the SOA

Received: October 30, 2016

Revised: January 16, 2017

Published: January 18, 2017

Table 1. Experimental Conditions for the SOA Samples Prepared from α -Pinene (APIN) and α -Humulene (HUM)

VOC precursor	oxidant	initial VOC (ppb)	initial O ₃ (ppb)	initial NO (ppb)	reaction time (h)	SOA concentration (mg/m ³)	collection time (h)	SOA collected (mg)
APIN	O ₃	500	640	<5	1	1.5	3	1.8
APIN	OH/NO _x	500	<5	300	2	0.18	3	0.24
APIN	NO ₃	1000	720	300	1	1.2	3	2.7
HUM	O ₃	500	660	<5	1.5	1.2	3	1.3
HUM	OH/NO _x	500	<5	300	1	0.87	4	1.1
HUM	NO ₃	500	600	300	1	1.8	3	4.1

produced by night-time chemistry would quickly change its composition after sunrise. One of the motivations for this work is to test this hypothesis.

Monoterpenes (C₁₀H₁₆) are the major precursors of SOA. Formation of SOA from monoterpenes, such as α -pinene, has been extensively documented, especially for the OH- and O₃-initiated oxidation pathways.^{11–17} Several studies have examined the oxidation of monoterpenes by the nitrate radical (NO₃).^{11,14,18–29} The NO₃-driven oxidation mechanism appears to be a major sink for BVOC and a major source for SOA at night in regions characterized by elevated NO_x (NO + NO₂) and O₃ levels.^{11,30}

Sesquiterpenes, such as α -humulene, are less abundant in ambient air than monoterpenes.³¹ However, their higher molecular weights and higher reactivity toward ozone and OH^{32–34} make them more efficient SOA precursors compared to the monoterpenes in terms of the SOA mass yields.^{25,35} There have been limited studies on the NO₃ oxidation of sesquiterpenes. Canosa-Mas et al.²⁶ and Shu and Atkinson³³ measured the rate constants for the reactions between selected sesquiterpenes and NO₃ radical. Fry et al.²³ investigated the NO₃ oxidation of β -caryophyllene, observing high SOA yields with a low organonitrate yield in the condensed phase. Jaoui et al. observed efficient SOA formation in reactions of several sesquiterpenes with NO₃.²⁵

Though numerous studies of each oxidation pathway (OH, O₃, or NO₃) have been performed for both monoterpenes and sesquiterpenes, only one study has attempted to systematically compare all three oxidation conditions for the same VOC precursor.²⁵ The first goal of our work is to compare the SOA formed in an environmental chamber from a model monoterpene (α -pinene) and a model sesquiterpene (α -humulene) under these three oxidation conditions. By using electrospray ionization high-resolution mass spectrometry (ESI-HRMS), we detect a much broader array of SOA compounds than previously observed and investigate the effect of the oxidation conditions on the molecular distribution of the SOA products. The second goal of this work is to examine the effect of photolysis on the molecular composition of SOA produced by NO₃ oxidation. Our results suggest facile photolysis of dissolved SOA compounds, especially the nitrogen-containing organic compounds (NOC). On the basis of the elemental composition assignments inferred from the ESI-HRMS data, we predict that photolysis should increase the volatility of SOA compounds based on a recently proposed “molecular corridors” parametrization^{36,37} between the molecular composition and volatility.

MATERIAL AND METHODS

Secondary Organic Aerosol Generation. SOA was prepared in a similar manner as previously described for the O₃ and photooxidation experiments.^{10,38} Briefly, into a 5 m³

chamber approximately 650 ppb of ozone was added for ozonolysis experiments, whereas approximately 300 ppb of nitric oxide and 2 ppm of hydrogen peroxide were added for photooxidation experiments. H₂O₂, added to the chamber by evaporation of its 30 v/v% aqueous solution with a stream of zero air, was used to generate the hydroxyl radical. Initial mixing ratios of α -pinene (APIN) and α -humulene (HUM) were 500 ppb for all experiments, except for the APIN/NO₃ experiment, in which the concentration of APIN was increased to 1000 ppb. For OH + NO_x experiments, UV–B lamps (FS40T12/UVB, Solarc Systems Inc.) were turned on and photooxidation time was 2 h for α -pinene experiments and 1 h for α -humulene experiments. To simulate the nighttime NO₃ radical chemistry, approximately 2-fold excess O₃ was added to 300 ppb NO to drive the following reactions:



After that, either α -pinene or α -humulene was added to the chamber. All experiments were performed under dry conditions at 21–25 °C and in the absence of seed particles. All chemicals noted above were purchased from Sigma-Aldrich at highest available stated purities and used without further purification.

SOA formed in the chamber were monitored by a TSI model 3936 scanning mobility particle sizer (SMPS), O₃ was monitored using a Thermo Scientific model 49i ozone analyzer, and a Thermo Scientific model 42i-Y NO_y analyzer recorded NO/NO_y data. The particles were collected through an activated carbon denuder at 17 SLM (standard liters per minute) onto poly(tetrafluoroethylene) (PTFE) filters (Millipore 0.2 μm pore size). We had to use high concentrations of precursors to collect a sufficient amount of SOA material (>0.2 mg) for both photochemical and control experiments (Table 1). Although the chemical composition of SOA formed at the high precursor and oxidant concentrations is not the same as that formed at ambient concentrations,³⁹ the major products as well as the degrees of chemical complexity of SOA should be comparable. Therefore, these SOA samples should be suitable for studying the general features of the photodegradation process. The filters were vacuum-sealed and immediately frozen at –20 °C in anticipation for offline aqueous photolysis experiments and mass spectrometry analysis.

Electrospray Ionization High-Resolution Mass Spectrometry (ESI-HRMS) of Aqueous Photolysis and Control Samples. Filter SOA samples were thawed and extracted in 6 mL of water (Fluka, HPLC grade) by sonicating the filter immersed in water. The extract was split in two equal portions, where 3 mL of the sample was used for photolysis experiments and 3 mL was used as a dark control. SOA material from α -pinene was believed to be fully dissolved during the extraction

on the basis of our previous experience.¹⁰ SOA material from α -humulene is less soluble in water,¹⁰ and only water-soluble components of SOA ended up in the solution. We did not have a way to quantify the amount of SOA remaining on the filter. The concentrations of the resulting solutions (up to 0.7 g/L if fully extracted) are more relevant to fog than to cloud droplets, so the conclusions reached in this paper should be more applicable to aqueous processes in a polluted environment than to those in a remote atmosphere. The solutions were used as soon as they were prepared. For photolysis experiments, the samples were photolyzed by a Xenon UV lamp (Newport model 66905) with a U-330 bandpass filter (Edmund optics #46-438) to reduce the visible and IR radiation. The temperature of the solution was not controlled but the solution did not measurably warm up above the room temperature during photolysis. The solution was open to air allowing oxygen to enter and volatile photolysis products to escape. The spectrum of the resulting radiation was recorded using a portable UV-vis spectrometer (Ocean Optics, USB4000) with most of the radiation falling in the 280–400 nm range. An azoxybenzene actinometer was used under the same experimental conditions to determine the flux of the lamp as described by Lignell et al.⁴⁰ On the basis of the actinometry measurements, we estimate that 1 h of photolysis with our lamp was equivalent to 16 h of photolysis by the overhead sun (SZA of 0° using the “Quick TUV”⁴¹ calculator with the following parameters: 300 Dobson overhead ozone, surface albedo of 0.1, ground elevation and altitude = 0 km). Even though the irradiation source had considerably stronger UV flux than the ambient sunlight, it was still far below the intensity needed to drive nonlinear processes in the solution, such as two-photon absorption.

The photolysis was carried out for a total of 4 h; the control samples remained in water for the same duration of time but were not exposed to radiation. Small aliquots (~300 μ L) were withdrawn from the sample and control cuvettes once an hour and analyzed by ESI-HRMS in a direct infusion mode. Immediately before the analysis, the extracted aliquot was mixed with acetonitrile in a 1:1 ratio to provide a more stable electrospray ionization. An LTQ-Orbitrap mass spectrometer (Thermo Corp.) equipped with a modified ESI source was used to analyze samples before and after photolysis.^{8–10,38,42–45} Mass spectra of the solvent (water + acetonitrile) were also collected to subtract from the sample mass spectra during data analysis. Mass spectra were acquired in the positive ion mode for all samples with a resolving power of 10^5 at m/z 400.

Analysis of the mass spectra was performed similarly to our previous work.^{5,10} Decon2LS (<https://omics.pnl.gov/software/decontools-decon2ls>) was used to generate a list of peak positions and abundances for each spectrum. The resulting peak lists for all the files in the same experimental batch (0, 1, 2, 3, and 4 h of photolysis, 0, 1, 2, 3, and 4 h of dark hydrolysis, and solvent blank) were clustered together. The clustered peaks were first assigned with a m/z tolerance of ± 0.001 to molecular formulas $C_cH_hO_oN_nNa_{n-1}^+$ (c, h, o, n refer to the number of corresponding atoms in the ion; the number of Na atoms was restricted to 0 or 1). We limited n to 3, and allowed for the presence of N atoms in the APIN/O₃ and HUM/O₃ assignments to see whether any nitrogen-containing impurities affected our measurements. Constraints were imposed on the elemental ratios ($0.0 < O/C < 1.3$, $0.7 < H/C < 2.0$) to eliminate unphysical assignments.⁴⁶ Peaks that corresponded to ¹³C isotopes and obvious impurities with anomalous mass

defects were excluded from further analysis. The set of the initially assigned peaks was used to internally recalibrate the m/z axis, and the mass spectra were then reassigned with a lower m/z tolerance of ± 0.00075 . The remaining peaks that could not be assigned within these constraints and peaks with ambiguous assignments were assigned manually with help of a molecular formula calculator (<http://magnet.fsu.edu/~midas/>). The majority of the observed ions corresponded to sodium ion adducts ($C_cH_hO_oN_nNa^+$); protonated molecules ($C_cH_hO_oN_nH^+$) generally had small abundances. For the remainder of this paper, we present and discuss formulas corresponding to the neutral species, $C_cH_hO_oN_n$, obtained by removing Na^+ or H^+ from the assigned ion formulas.

“Molecular Corridors” Analysis of the SOA Volatility Distribution. The volatility distributions of SOA components were estimated using the “molecular corridor” approach, which takes advantage of an inverse correlation between pure compound saturation mass concentration (C_0) and molar mass of organic compounds.^{36,37} Recently, Li et al.³⁷ developed parametrizations to predict C_0 of organic compounds containing oxygen, nitrogen, and sulfur from the elemental composition. The ESI-HRMS data are well suited for this purpose because they provide an experimental distribution of molecular formulas (and hence, molecular weights) in the SOA sample. On the basis of the Pankow absorptive partitioning theory under the assumption of ideal thermodynamic mixing,^{47–49} the gas-phase mass concentration ($C_{g,i}$) and particle-phase mass concentration ($C_{p,i}$) of compound i are related as follows

$$\frac{C_{g,i}}{C_{p,i}} = \frac{C_{0,i}}{C_p} \quad (1)$$

where C_p is the total mass concentration of organic particulate matter. Compounds for which $C_{0,i}$ is smaller than C_p should reside predominantly in the particle phase at equilibrium. We note that the above expression does not account for nonideal thermodynamic mixing of compounds in particles. The term “volatility” often refers to the effective saturation mass concentration (C^*), which is related to C_0 via an unknown activity coefficient, $C^* = \gamma \times C_0$. C^* and C_0 are interchangeable under the assumption of an ideal thermodynamic mixing ($\gamma = 1$).

Because we generated SOA at high concentrations (Table 1) and because of possible filter artifacts (volatile compounds partitioning in the SOA material and on the filter), the SOA samples contained compounds that would be expected to evaporate from particles under typical ambient conditions. Therefore, for each SOA sample we calculated a fraction of the observed compounds with $C_{0,i}$ below $C_p = 10 \mu\text{g m}^{-3}$, a value that is representative of moderately polluted air, from the observed relative abundances in the ESI-HRMS mass spectra, ESI_i .

$$\text{fraction} = \frac{\sum ESI_i(C_{0,i} < C_p)}{\sum ESI_i} \quad (2)$$

Equation 2 assumes that the mass fraction of each SOA compound is proportional to its observed relative abundance in the ESI-HRMS mass spectrum. This is certainly an approximation because ESI detection sensitivities depend strongly on the structures of the molecules and their surface activities.⁵⁰ Furthermore, the transmission of ions through the mass spectrometer and their detection efficiency strongly

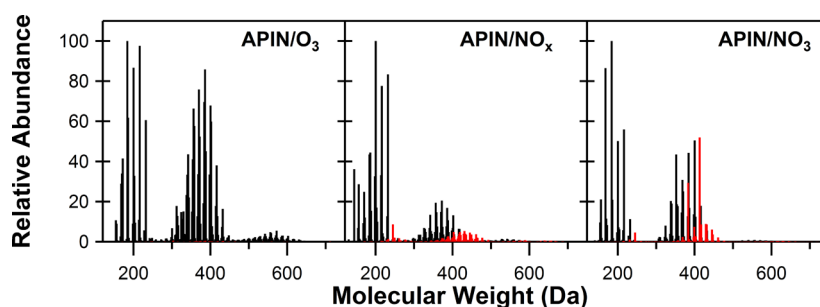


Figure 1. Mass spectra for the α -pinene (APIN) SOA samples formed under three oxidation conditions (ozonolysis, OH/NO_x photooxidation, and reaction with NO₃). The x -axis corresponds to the molecular weight of the neutral SOA compounds, and the y -axis corresponds to relative abundances in the ESI mass spectra. Peaks in red denote nitrogen-containing organic compounds (NOC).

Table 2. Top Five Peaks for α -Pinene SOA from Each Set of Oxidation Conditions

molecular formula	molecular weight	relative abundance (%)	formula (MW)	molecular weight	relative abundance (%)
	APIN/O ₃			HUM/O ₃	
C ₁₀ H ₁₆ O ₃	184	100	C ₁₅ H ₂₄ O ₇	316	100
C ₁₀ H ₁₆ O ₅	216	98	C ₁₅ H ₂₄ O ₆	300	49
C ₁₀ H ₁₆ O ₄	200	87	C ₁₅ H ₂₄ O ₄	268	29
C ₁₉ H ₃₀ O ₈	386	86	C ₁₅ H ₂₄ O ₅	284	25
C ₁₉ H ₃₀ O ₇	370	76	C ₁₅ H ₂₄ O ₈	332	18
C ₁₇ H ₂₆ O ₈	358	50 ^{at}			
	APIN/NO _x			HUM/NO _x	
C ₁₀ H ₁₆ O ₄	200	100	C ₁₅ H ₂₄ O ₆	300	100
C ₁₀ H ₁₆ O ₆	232	83	C ₁₅ H ₂₄ O ₇	316	60
C ₁₀ H ₁₆ O ₅	216	78	C ₁₄ H ₂₄ O ₆	288	47
C ₉ H ₁₄ O ₄	186	45	C ₁₅ H ₂₄ O ₅	284	44
C ₁₀ H ₁₆ O ₃	184	44	C ₁₅ H ₂₅ O ₈ N	347	34
C ₁₇ H ₂₆ O ₈	358	7 ^{at}			
	APIN/NO ₃			HUM/NO ₃	
C ₁₀ H ₁₆ O ₃	184	100	C ₁₅ H ₂₄ O ₇	316	100
C ₁₀ H ₁₆ O ₂	168	87	C ₁₅ H ₂₄ O ₆	300	54
C ₁₀ H ₁₆ O ₅	216	56	C ₁₅ H ₂₄ O ₅	284	46
C ₂₀ H ₃₁ O ₈ N	413	52	C ₁₅ H ₂₄ O ₄	268	41
C ₂₀ H ₃₂ O ₈	400	51	C ₁₄ H ₂₄ O ₆	288	27
C ₁₇ H ₂₆ O ₈	358	1 ^{at}			

^aEven though the “358-dimer” did not make it to the top-five list; we included it in this table because of the significant previous interest to this molecule.^{63,67–69}

depend on the instrumental configuration. However, for a given set of instrumental parameters, ESI tends to preferentially ionize larger molecules, and for homologous compounds, there is a positive correlation between the ESI detection sensitivity and molecular weight.⁵¹ Therefore, eq 2 should be a reasonable approximation of the mass fraction of the detected SOA compounds that should be associated with particles, especially for the purposes of comparing two samples analyzed under the same experimental conditions.

RESULTS AND DISCUSSION

Composition and Volatility of SOA before Photolysis.

The main purpose of this section is to compare the detailed molecular compositions of SOAs generated under three different oxidation conditions (ozonolysis, OH/NO_x photooxidation, NO₃ oxidation). Table 1 provides a list of the SOA samples produced in this work. The peak SOA concentration and the amount of the collected SOA varied between the different samples. The OH + NO_x photooxidation resulted in the lowest amount of SOA produced, whereas the NO₃ oxidation produced the most SOA. This is qualitatively

consistent with a previous report that found the average SOA yields for the same VOC precursor to be the highest for the NO₃ reaction;²⁵ however, the SOA yields could not be qualitatively compared because we did not measure the amount of reacted VOC.

The reaction of α -pinene with NO₃ was recently reported to produce unexpectedly low SOA yields compared to reactions of other monoterpenes with NO₃.^{22,23} Furthermore, ozonolysis was found to be much more efficient in nucleating new particles from α -pinene and β -pinene than reaction with NO₃ or OH.¹⁸ We were able to form particles for the APIN/NO₃ system using high concentrations of α -pinene in our system (1 ppm), in agreement with several previous studies.^{18,20,52}

Figure 1 shows the high-resolution mass spectra for α -pinene SOA from each oxidation experiment, and Table 2 lists the peaks with the highest relative abundances. The spectrum of APIN/O₃ in Figure 1 is similar to the previously reported spectra of monoterpene/O₃ SOA,^{10,53–57} with a distinct distributions of peaks in the monomeric range (<300 Da), dimeric range (300–500 Da), and trimeric range (500–700 Da), corresponding to products containing, one, two, or three

oxygenated α -pinene units, respectively. We allowed for the presence of nitrogen in the assignments but observed very few NOC (Figure 1), confirming that nitrogen-containing impurities were minor. The most abundant peaks corresponded to well-known monomeric products of α -pinene ozonolysis: $C_{10}H_{16}O_3$ (pinonic acid), $C_{10}H_{16}O_5$ (MW 216), and $C_{10}H_{16}O_4$ (10-hydroxypinonic acid).⁵⁸ The most likely identities for these products appear in parentheses next to the formulas. In many cases, a number of possible compounds can match the same formula. For example, the compound with MW = 216 was observed in refs 59–64 and assigned to a C10-carboxylic acid by Kahnt et al.⁵⁹ but to a peroxide by Venkatchari and Hopke⁶² and by Camredon et al.⁶³ The next two strongest peaks corresponded to dimeric compounds $C_{19}H_{30}O_8$ (MW 386) and $C_{19}H_{30}O_7$ (MW 370). Both of these dimers were previously reported in ozonolysis of α -pinene in refs 62 and 65, but they could not establish their structures on the basis of the fragmentation patterns. More recently, Kristensen et al.⁶⁶ detected both of these dimers, along with many others, in the lab and in the boreal forest measurement site of Hyytiälä, Finland, and suggested that they are ester compounds. These dimer species were also relatively prominent in negative ion mode high-resolution mass spectra reported by Putman et al.⁶⁴ The best characterized dimer in APIN/ O_3 is $C_{17}H_{26}O_8$ (MW 358),^{63,67–69} which corresponds to *cis*-pinic acid esterified with diaterpenylic acid. This dimer was also observed as an abundant peak in the APIN/ O_3 mass spectrum (50% of the pinonic acid peak); its abundance was much lower under the NO_x and NO_3 oxidation conditions.

The high-resolution mass spectrum of APIN/ NO_x SOA shown in Figure 1 is also qualitatively similar to the one we reported previously.¹⁰ In our previous work, many carbonyl and carboxyl SOA compounds reacted with the methanol extraction solvent and were observed as the corresponding hemiacetals and esters.¹⁰ In this study, we excluded methanol from the SOA extracting solution to avoid the formation of hemiacetals and esters. The major peaks in the spectra (Table 2) retained the C_{10} skeleton of α -pinene, as expected. The five most abundant peaks were monomeric products with formulas and most likely identities corresponding to $C_{10}H_{16}O_4$ (10-hydroxypinonic acid),⁵⁸ $C_{10}H_{16}O_6$ (MW 232), $C_{10}H_{16}O_5$ (MW 216), $C_9H_{14}O_4$ (pinic acid), and $C_{10}H_{16}O_3$ (pinonic acid). The MW 232 compound was previously attributed not only to diaterpenylic acid acetate⁷⁰ but also to a peroxide compound.⁶² The fraction of oligomers was substantially smaller in the APIN/ NO_x SOA than in the APIN/ O_3 SOA; for example, the 358-dimer was an order of magnitude lower in abundance in APIN/ NO_x SOA. The fraction of peaks corresponding to NOC was predictably higher in the APIN/ NO_x SOA. The NOC peaks also showed clear clustering into monomers, dimers, and trimers, with the average mass of each NOC cluster shifted by about 40–50 Da toward higher molecular weights compared to the nitrogen-free peaks. This could be interpreted as a result of adding an $-ONO_2$ group (MW 62) instead of an $-OH$ (MW 17) group to the molecule, resulting in a MW difference of 45. Indeed, most of the NOC in APIN/ NO_x are expected to be organonitrates on the basis of the mechanism of BVOC oxidation under high- NO_x conditions.

The high-resolution mass spectrum of APIN/ NO_3 SOA has not been reported before. The mass spectrum in Figure 1 is also clustered in the monomeric, dimeric, and trimeric compounds. The most abundant three peaks corresponded to $C_{10}H_{16}O_3$ (pinonic acid), $C_{10}H_{16}O_2$ (pinonaldehyde), and $C_{10}H_{16}O_5$

(MW 216). They were closely followed by dimeric compounds $C_{20}H_{31}O_8N$ (MW 413) and $C_{20}H_{32}O_8$ (MW 400). The 358-dimer mentioned above was barely detectable in the APIN/ NO_3 SOA mass spectrum in contrast to the APIN/ O_3 SOA case.

The most striking difference between the APIN/ NO_3 SOA and APIN/ NO_x SOA was a much higher fraction of NOC in the former. For example, Table 3 shows that the fraction of

Table 3. Percent Fraction of NOC Observed in APIN SOA and HUM SOA Samples

	APIN/ O_3	APIN/ NO_x	APIN/ NO_3	HUM/ O_3	HUM/ NO_x	HUM/ NO_3
0N ^a	95%	64%	56%	92%	54%	63%
1N	5%	36%	27%	8%	37%	19%
2N			12%		6%	15%
3N			5%		3%	3%

^a0N, 1N, 2N, and 3N correspond to compounds with 0 ($C_xH_yO_z$), 1 ($C_xH_yO_zN$), 2 ($C_xH_yO_zN_2$), and 3 ($C_xH_yO_zN_3$) nitrogen atoms, respectively.

peaks containing 0, 1, 2, and 3 nitrogen atoms shifted toward higher N atom values from ozonolysis to OH/ NO_x photo-oxidation to NO_3 oxidation. This is expected because NO_3 can react with α -pinene directly by addition to the double bond producing NOC already in the first generation of products. It is interesting that NOC clearly prevailed in the dimeric products and were absent from monomeric products of α -pinene oxidation. For example, one of the major peaks in the spectrum was a dimer $C_{20}H_{31}O_8N$ (Table 2). The NOC monomeric species could be too volatile to partition into the aerosol, which could explain why little SOA is formed at lower α -pinene concentrations.^{22,23}

Figure 2 shows the mass spectra of HUM SOA produced under different oxidation conditions, and Table 2 lists the top five peaks observed in the mass spectra. The majority of the detected compounds were monomers retaining the C_{15} skeleton of α -humulene, but products with C-numbers differing from 15 in humulene were also observed. Major peaks for all three sets of oxidation conditions were dominated by $C_{15}H_{24}O_6$ compounds with *o* ranging from 4 to 8. Of these compounds, only $C_{15}H_{24}O_4$ has been previously identified as α -humuladionic acid.^{71,72} Some of the major compounds had 14 carbon atoms, with one carbon atom lost from the initial humulene structure. Unlike the APIN case, there were not many oligomeric species in mass spectra. Even the first generation products of oxidation of sesquiterpenes are sufficiently involatile that they can form SOA without having to dimerize first.⁷³ NOC were present at the small level of impurities in the HUM/ O_3 SOA sample, as expected. The fractions of NOC were comparable in the HUM/ NO_x and HUM/ NO_3 SOA samples (Table 3). Again, the shift in the average molecular weight of the NOC and nitrogen-free compounds was consistent with formation of organonitrates; for example, $C_{15}H_{25}O_8N$ (MW 347) listed in the top-five peaks in the HUM/ NO_x SOA in Table 2 could be a result of a replacement of an $-OH$ group by $-ONO_2$ group in $C_{15}H_{26}O_6$ (MW 302, which was also present in the mass spectrum with a relative abundance of 11%).

Photolysis-Induced Changes in Molecular Composition. Figure 3 shows the mass spectra of SOA samples during photolysis and control experiments for the 0 and 4 h reaction

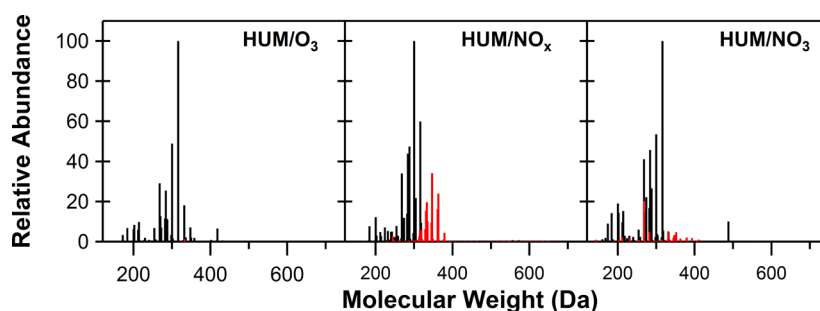


Figure 2. Mass spectra for the α -humulene SOA samples formed under three oxidation conditions (ozonolysis, NO_x photooxidation, and reaction with NO_3) before photolysis. The x -axis corresponds to the molecular weight of the neutral SOA compounds, and the y -axis corresponds to relative abundances in the ESI mass spectra. Peaks in red denote NOC.

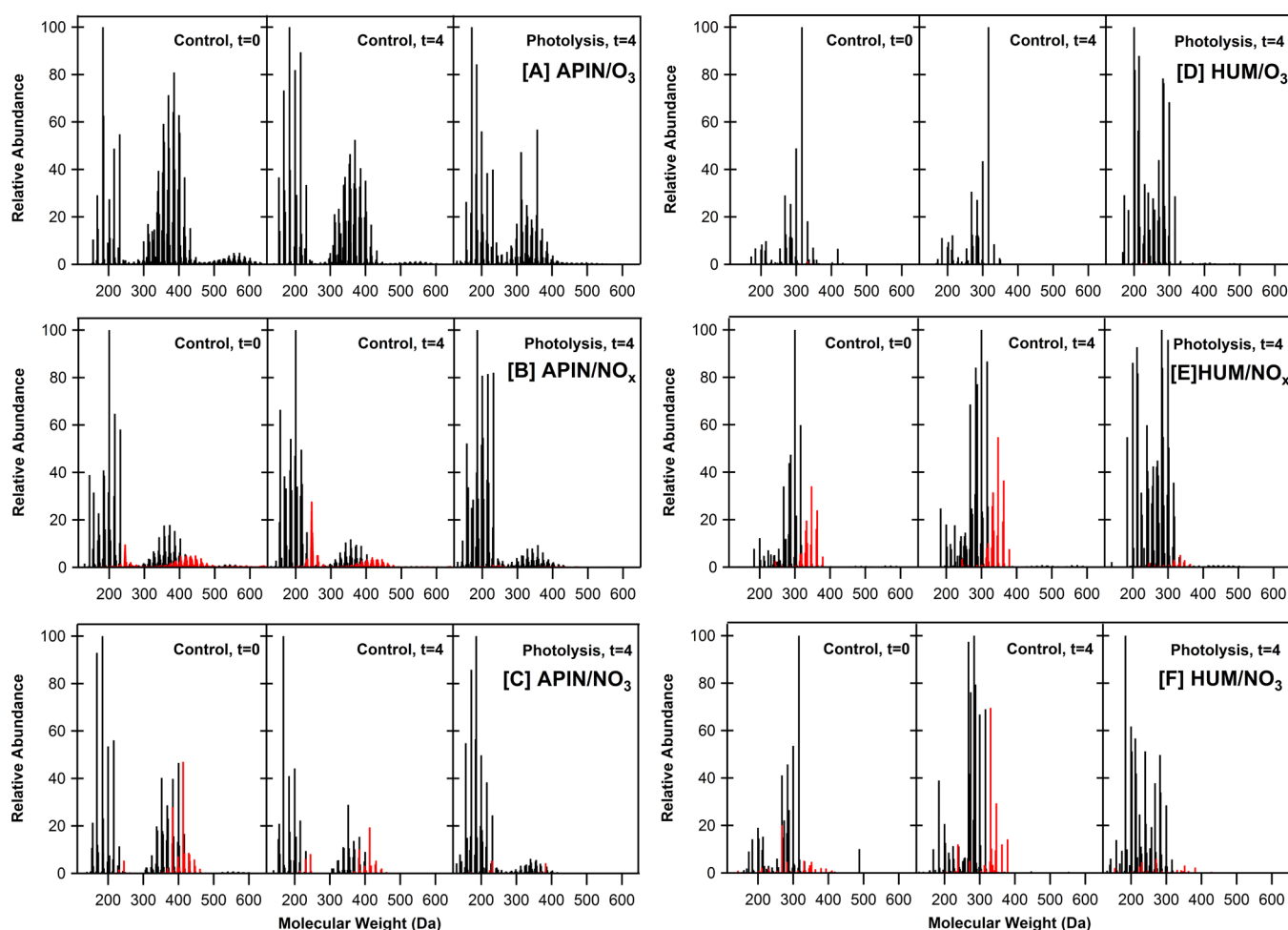


Figure 3. High-resolution mass spectra of the APIN/ O_3 [A], APIN/ NO_x [B], APIN/ NO_3 [C], HUM/ O_3 [D], HUM/ NO_x [E], and HUM/ NO_3 [F] aqueous SOA extracts at $t = 0$ h, the dark control after 4 h, and the photolysis sample after 4 h ($t = 4$). The x -axis corresponds to the molecular weight of the neutral compounds and the y -axis corresponds to the relative abundance in the positive ion mode ESI mass spectrum. Peaks are normalized with respect to the largest peak in the sample. Red peaks denote NOC.

time (1, 2, and 3 h mass spectra are omitted to avoid cluttering the figure). The mass spectra changed significantly upon photolysis in several important aspects. The first obvious conclusion from Figure 3 is that the higher molecular weight (MW) compounds were converted to lower MW compounds by photolysis. This is especially noticeable for SOA derived from α -pinene: the photolysis reduced the abundance of the dimeric species relative to the monomeric ones and obliterated all of the trimeric species.

In control samples, hydrolysis also reduced the relative abundance of the dimeric and trimeric species (Figure 3). At first glance, the effect of hydrolysis on the oligomers appeared to be much smaller than that of photolysis. However, we should keep in mind that photolysis was done with a light source that was 16 times stronger than solar radiation, so 4 h under the lamp was approximately equivalent to 64 h under the sun. Extrapolating the 4 h control experiments suggests that the effect of hydrolysis could be comparable to the effect of photolysis.

The most obvious effect of photolysis was the dramatic removal of NOC species. They were removed almost entirely for the mixtures of APIN/NO_x and APIN/NO₃ SOA. The reduction in the number of the NOC species was also obvious for the HUM/NO_x and HUM/NO₃ SOA, although a few NOC appeared to persist. The hydrolysis in the control samples did not have the same effect; the relative amount of NOC remained about the same, or even increased in some cases, judging from the relative peak abundance.

Aerosol mass spectrometer (AMS) measurements of average elemental ratios (H/C, O/C, and N/C) are frequently reported in both field and lab studies.⁷⁴ To aid in the comparison with other experiments, we calculated the average elemental ratios, as well as the average molecular size (denoted by the number of C atoms per molecule), and average double bond equivalent (DBE) from the assigned, neutral molecular formulas. All averaged quantities were calculated with respect to peak abundances for all observed compounds as shown below:

$$\langle X \rangle = \frac{\sum I_i x_i}{\sum I_i} \quad (x = c, o, h, n, \text{DBE}) \quad (3)$$

$$\frac{\langle X \rangle}{\langle Y \rangle} = \frac{\sum I_i x_i}{\sum I_i y_i} \quad (x, y = o, c, h, n) \quad (4)$$

The results from these calculations for the control and photolysis samples are compiled in Figures 4 and 5 for APIN SOA and HUM SOA, respectively, as a function of the photolysis (or hydrolysis) time from 0 to 4 h.

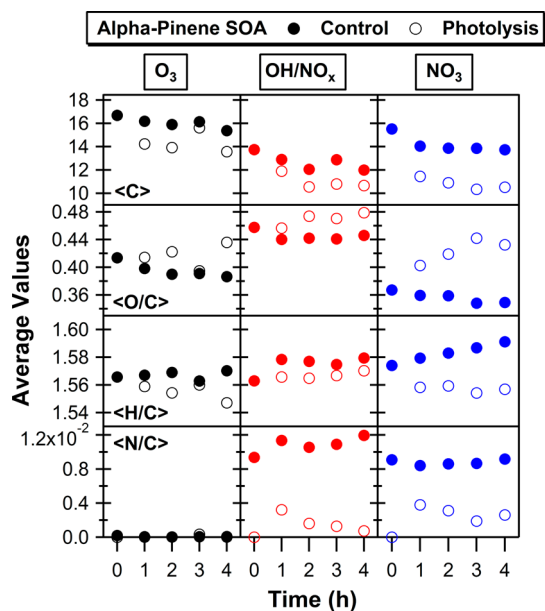


Figure 4. Time-dependent average number of carbon atoms and elemental ratios in the photolysis (open circles) and dark control samples (closed circles) for each of the α -pinene oxidation conditions.

The average molecular size shown in Figures 4 and 5 was approximately the same for all SOA samples, with $\langle C \rangle$ falling in the range of 14–16. This happened because monomer (C10) and dimer (C20) compounds were equally represented for α -pinene SOA (Figure 1), but the α -humulene SOA was dominated by the monomer compounds (Figure 2). There was a clear trend in the reduction of $\langle C \rangle$ with photolysis, which agreed with the observation that high-MW oligomers were

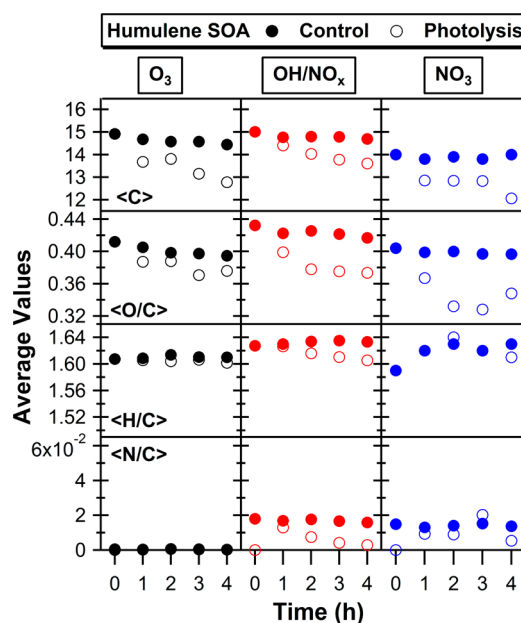
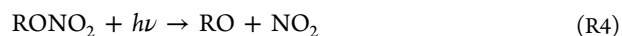


Figure 5. Time-dependent average number of carbon atoms and elemental ratios in the photolysis (open circles) and dark control samples (closed circles) for each of the α -humulene oxidation conditions.

degraded, as reflected in the mass spectra shown in Figure 3. In our previous work on photolysis of SOA solutions, we also observed a reduction in the average molecular size for a broad range of SOA.^{8–10} The average molecular size was also reduced by hydrolysis. The effect of the hydrolysis was smaller than that of photolysis, but as pointed out above, the photolysis was accelerated in our experiments by the elevated actinic flux from the lamp. As a result, both photolysis and hydrolysis could have comparable effects on the reduction of the average molecular size under ambient solar irradiation conditions.

The average O/C ratio traditionally describes the degree of oxidation of a compound. For all the APIN samples, we observed an increase in the average O/C during photolysis, and a decrease in O/C during hydrolysis. This is consistent with previous aqueous photolysis studies of natural organic matter,^{75,76} and aqueous SOA samples.^{8–10} In contrast, we observed a decrease in the average O/C for HUM samples, during both the photolysis and hydrolysis. This difference in behavior between APIN and HUM SOA implies that the effect of aqueous processing of SOA on the average O/C may be different for different types of SOA.

Romonosky et al. previously reported an efficient depletion of NOC species in photolysis of different SOA prepared under high NO_x conditions.¹⁰ In the present study, the average N/C ratio for samples made in the presence of NO_x and NO₃ also decreased dramatically with photolysis. We attribute these observations to photolysis of organonitrates



with secondary processes forming stable nitrogen-free compounds from RO radicals. Organonitrates are relatively weak absorbers of near-UV radiation.⁷⁷ However, multifunctional compounds found in SOA are expected to be stronger absorbers and more photochemically active.⁷⁸ Some, but not all, of the NOC species appeared to be reduced in control samples as well, which is consistent with facile hydrolysis of

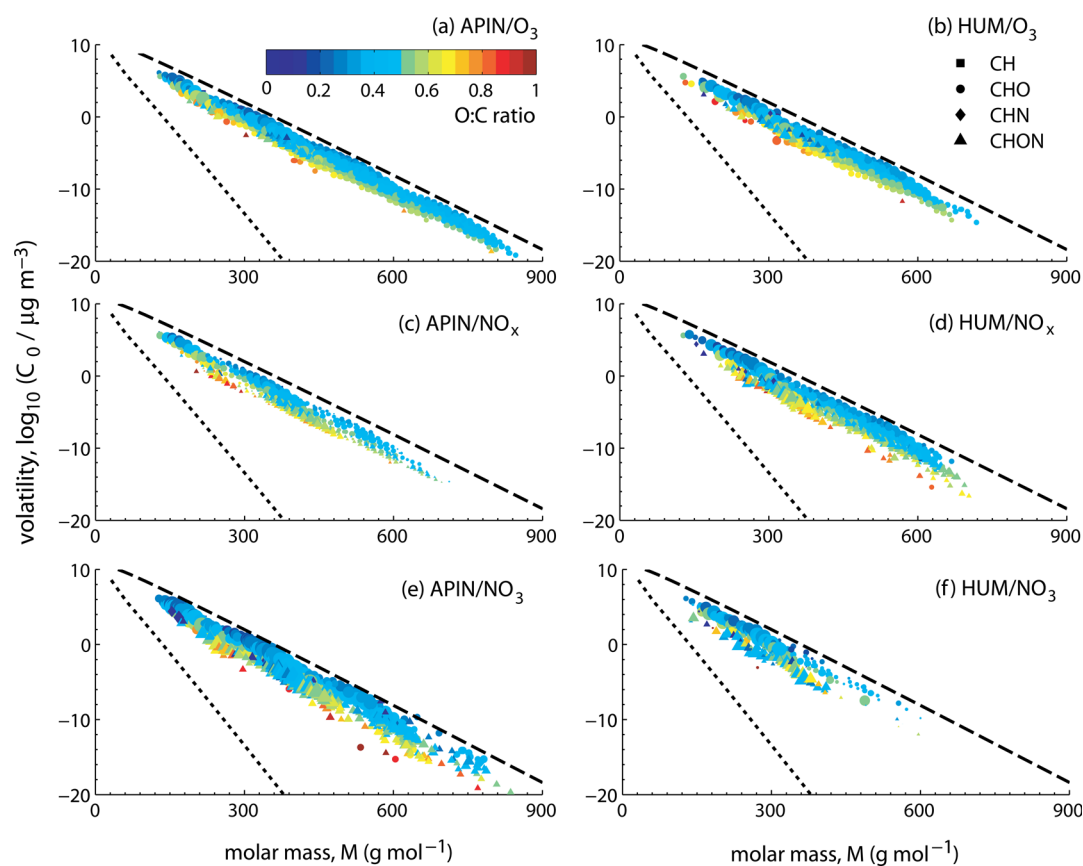


Figure 6. Calculated volatility distributions for the observed SOA compounds before photolysis. The upper dashed line represents linear alkanes C_nH_{2n+2} with $O:C = 0$ and the lower dotted line represents linear sugar alcohols $C_nH_{2n+2}O_n$ with $O:C = 1$. The markers represent individual compounds color-coded by the $O:C$ ratio. The sizes of the markers are logarithmically scaled by mass spectral abundances.

certain secondary and tertiary organic nitrates, but not the primary ones.^{79–81} The average N/C was relatively insensitive to the hydrolysis.

The mechanism of the observed photodegradation of SOA compounds, including organonitrates, cannot be conclusively proven because it is challenging to distinguish between direct photolysis of organic compounds and their indirect photo-oxidation by OH . Hydroxyl radicals can be formed as byproducts of SOA photolysis⁸² or even from the spontaneous decomposition of SOA compounds in water.^{82,83} In the experiments described in this paper, we did not intentionally add any OH precursors to the photolyzed solutions to emphasize direct photolysis. Aljawhary et al.⁸⁴ examined OH -driven aqueous photooxidation of pinonic acid, which photolyzes too slowly,⁴⁰ and of two other surrogate products of α -pinene oxidation. They observed formation of less volatile products in these processes. For example, more aerosol could be produced by atomization of a solution of pinonic acid and H_2O_2 after the solution was irradiated. We tested the effect of OH in a separate series of experiments, in which hydrogen peroxide or nitrate ion were intentionally added to the same SOA solutions and found that the photodegradation of SOA organics occurred at an even faster rate, as judged by the relative abundance of the dimer species to the monomer species in the mass spectrum after 4 h of irradiation (the data are not shown because they are qualitatively similar to the data shown in Figure 3). The SOA compounds that are removed under our experimental conditions may already be sufficiently oxidized making the fragmentation-type processes more favorable,^{85–87}

regardless of the mechanism (photolysis, hydrolysis, OH oxidation).

Effect of Photolysis on SOA Volatility. Figure 6 shows the distribution of pure compound saturation vapor pressures for the fresh SOA (before photolysis) estimated by the “molecular corridors” approach. The volatilities of fresh SOA compounds spanned a broad range with predicted values as low as $10^{-20} \mu\text{g m}^{-3}$. A number of volatile compounds were also observed in the particles with volatilities up to $\log(C_0) = 6$ (Figure 6). The compounds should not be present in ambient particles on the basis of an equilibrium partitioning assumption. The reason we observed them in our experiments could be because they were physically or chemically trapped in the particles due to kinetic limitations⁸⁸ or were enhanced in the particles due to the high concentrations used in SOA preparation.

The reaction of α -pinene with NO_3 was observed to make almost no SOA under low-concentration conditions.^{22,23} However, under the higher concentration conditions of this work, the APIN/ NO_3 SOA contained a number of compounds with saturation vapor pressure below $1 \mu\text{g m}^{-3}$ (Figure 6) and was not qualitatively different from the APIN/ O_3 and APIN/ NO_x volatility distributions.

The observation of extensive fragmentation of SOA compounds by photolysis and the resulting reduction in their average molecular weight suggests that SOA may become more volatile as its components are fragmented by radiation. We attempted to estimate the effect of photolysis on the particle volatility using the “molecular corridors” parametrization. Table

4 lists the mass fraction of the SOA compounds expected to reside in particle phase at $C_p = 10 \mu\text{g}/\text{m}^3$ calculated from eq 2.

Table 4. Percent Mass Fractions of Observed SOA Compounds with Saturation Vapor Pressures (C_0) below $10 \mu\text{g}/\text{m}^3$ before and after Photolysis and Hydrolysis

SOA	0 h photolysis	4 h photolysis	0 h hydrolysis	4 h hydrolysis
APIN/ O_3	70	52	71	62
APIN/ NO_x	48	19	48	36
APIN/ NO_3	56	17	61	45

A reduction in this fraction would mean that the compounds in the SOA sample become more volatile. The data show that both the photolysis and hydrolysis reduced the fraction of material residing in the particle phase. The effect appeared to be stronger for photolysis. For example, for the APIN/ NO_x SOA, the fraction of the detected compounds expected to be in the particle phase went down from about 50% to less than 20% after photolysis, and down to 36% during hydrolysis. As pointed out earlier, the rate of photolysis was accelerated by the stronger actinic flux from the lamp compared to normal ambient conditions, so it can be concluded that both photolysis and hydrolysis had comparable influences on the increase of SOA volatility. Both processes produced smaller, more volatile compounds from larger, less volatile ones initially present in SOA.

CONCLUSIONS AND IMPLICATIONS

This study presented high-resolution mass spectra of SOA prepared from a common monoterpene α -pinene and a common sesquiterpene α -humulene oxidized under three different conditions: ozonolysis, reaction with OH in the presence of NO_x , and reaction with NO_3 . Molecular formulas could be assigned to most of the observed peaks, and the major observed peaks were consistent with previous studies of SOA from these two precursors. The SOA contained a mixture of monomeric and oligomeric products in the case of α -pinene; it was dominated by monomeric products $\text{C}_{15}\text{H}_{24}\text{O}_o$ with $o = 4-8$ in the case of α -humulene. The SOA prepared under OH/ NO_x and NO_3 oxidation conditions had a number of nitrogen-containing organic compounds (NOC), assumed to be organonitrates, RONO_2 .

The composition of SOA changed significantly during aqueous photolysis. The photolysis time used in these experiments was rather long (4 h of photolysis under the experimental conditions; approximately equivalent to 64 h under sunlight) but the changes were clearly visible already after 1 h of photolysis. Two most obvious effects were the reduction in the average molecular size due to the preferential degradation of oligomeric compounds, and strong reduction in the amount of nitrogen-containing organic compounds. The NOC were almost completely absent after 4 h of photolysis under the experimental conditions, which was approximately equivalent to 64 h under sunlight. In contrast, most (but not all) NOC persisted in aqueous solutions under dark conditions. The main implication of this work is that organonitrates derived from BVOC oxidation are not likely to survive long-range transport of SOA when aqueous processing is occurring under sunlit conditions. Hydrolysis of organonitrates was suggested as the reason between much lower amounts of organonitrates detected in field compared to lab studies;⁸¹ photolysis could be

just as important, if not more important, in removing these compounds. The photodegradation and hydrolysis of NOC observed in this work could potentially be responsible for the facile (time scale of 2–4 h) removal of highly functionalized organonitrates observed in recent field measurements in the southeast United States.⁸⁹

Although this study focused on aqueous photochemistry, similar photodegradation processes could potentially be effective in the gaseous phase and in organic particles, in the absence of liquid water. However, the differences in the mechanisms and rates of photochemical processes occurring inside the organic phase of SOA and in an aqueous solution of SOA is still an open question. Although the SOA material is known to photodegrade at atmospherically relevant rates,⁹⁰ certain types of photochemical processes are suppressed by the viscous environment of the SOA material.^{91,92} Another complication is that we only tracked water-soluble components of SOA in this study, and the water-insoluble fraction that remained on the filter could have very different photochemistry. The matrix effect on the photodegradation of SOA compounds should be examined in future experiments.

Aqueous photochemical processing of organics is viewed as an important source of SOA.^{6,7} For example, it is well-established that small water-soluble molecules such as glyoxal and methylglyoxal produce low-volatility products through oxidation and oligomerization processes.^{93–95} Our experiments clearly demonstrate that not all aqueous processes lead to buildup of SOA by generating low-volatility products; there are also competing hydrolysis and photolysis processes that make dissolved organic compounds smaller and more volatile. Therefore, an SOA particle entering a fog or cloud droplet could potentially shrink after the droplet evaporates. We should stress that in our experiments we removed the volatile compounds from the aerosol before dissolving the particles in water. The situations in which both small water-soluble molecules and particulate compounds are scavenged by water droplets, and then irradiated by sunlight, will be more complex. Will the photodegradation of larger SOA compounds prevail over oligomerization and OH oxidation of smaller ones? It will be an interesting question to explore in future studies.

ASSOCIATED CONTENT

Supporting Information

The Supporting Information is available free of charge on the ACS Publications website at DOI: 10.1021/acs.jpca.6b10900.

List of the observed peaks and their formula assignments in the fresh SOA samples (XLSX)

AUTHOR INFORMATION

Corresponding Author

*S. A. Nizkorodov. Phone: 949-824-1262. E-mail nizkorod@uci.edu.

ORCID

Sergey A. Nizkorodov: 0000-0003-0891-0052

Notes

The authors declare no competing financial interest.

ACKNOWLEDGMENTS

We acknowledge support by the U.S. Department of Commerce, National Oceanic and Atmospheric Administration through Climate Program Office's AC4 program, awards

NA13OAR4310066 (PNNL) and NA13OAR4310062 (UCI). D.E.R. thanks NSF for the support via the graduate fellowship program and NSF grant AGS-1227579. The ESI-HRMS measurements were performed at the W. R. Wiley Environmental Molecular Sciences Laboratory (EMSL)—a national scientific user facility located at PNNL, and sponsored by the Office of Biological and Environmental Research of the U.S. DOE. PNNL is operated for U.S. DOE by Battelle Memorial Institute under Contract No. DE-AC06-76RL0 1830.

REFERENCES

- (1) Finlayson-Pitts, B. J.; Pitts, J. N. *Chemistry of the Upper and Lower Atmosphere: Theory, Experiments, and Applications*; Academic Press: San Diego, 2000.
- (2) George, C.; Ammann, M.; D'Anna, B.; Donaldson, D. J.; Nizkorodov, S. A. Heterogeneous Photochemistry in the Atmosphere. *Chem. Rev.* **2015**, *115*, 4218–4258.
- (3) Rudich, Y.; Donahue, N. M.; Mentel, T. F. Aging of Organic Aerosol: Bridging the Gap between Laboratory and Field Studies. *Annu. Rev. Phys. Chem.* **2007**, *58*, 321–352.
- (4) Pöschl, U.; Shiraiwa, M. Multiphase Chemistry at the Atmosphere–Biosphere Interface Influencing Climate and Public Health in the Anthropocene. *Chem. Rev.* **2015**, *115*, 4440–4475.
- (5) Nizkorodov, S. A.; Laskin, J.; Laskin, A. Molecular Chemistry of Organic Aerosols through the Application of High Resolution Mass Spectrometry. *Phys. Chem. Chem. Phys.* **2011**, *13*, 3612–3629.
- (6) Evens, B.; Turpin, B. J.; Weber, R. J. Secondary Organic Aerosol Formation in Cloud Droplets and Aqueous Particles (aqSOA): A Review of Laboratory, Field and Model Studies. *Atmos. Chem. Phys.* **2011**, *11*, 11069–11102.
- (7) Herrmann, H.; Schaefer, T.; Tilgner, A.; Styler, S. A.; Weller, C.; Teich, M.; Otto, T. Tropospheric Aqueous-Phase Chemistry: Kinetics, Mechanisms, and Its Coupling to a Changing Gas Phase. *Chem. Rev.* **2015**, *115*, 4259–4334.
- (8) Bateman, A. P.; Nizkorodov, S. A.; Laskin, J.; Laskin, A. Photochemical Processing of Secondary Organic Aerosols Dissolved in Cloud Droplets. *Phys. Chem. Chem. Phys.* **2011**, *13*, 12199–12212.
- (9) Nguyen, T. B.; Laskin, A.; Laskin, J.; Nizkorodov, S. A. Direct Aqueous Photochemistry of Isoprene High-NO_x Secondary Organic Aerosol. *Phys. Chem. Chem. Phys.* **2012**, *14*, 9702–9714.
- (10) Romonosky, D. E.; Laskin, A.; Laskin, J.; Nizkorodov, S. A. High-Resolution Mass Spectrometry and Molecular Characterization of Aqueous Photochemistry Products of Common Types of Secondary Organic Aerosols. *J. Phys. Chem. A* **2015**, *119*, 2594–2606.
- (11) Atkinson, R.; Arey, J. Gas-Phase Tropospheric Chemistry of Biogenic Volatile Organic Compounds: A Review. *Atmos. Environ.* **2003**, *37*, S197–S219.
- (12) Lee, A.; Goldstein, A. H.; Keywood, M. D.; Gao, S.; Varutbangkul, V.; Bahreini, R.; Ng, N. L.; Flagan, R. C.; Seinfeld, J. H. Gas-Phase Products and Secondary Aerosol Yields from the Ozonolysis of Ten Different Terpenes. *J. Geophys. Res.* **2006**, *111*, 10.1029/2005JD006437.
- (13) Calogirou, A.; Larsen, B. R.; Kotzias, D. Gas-Phase Terpene Oxidation Products: A Review. *Atmos. Environ.* **1999**, *33*, 1423–1439.
- (14) Hoffmann, T.; Odum, J. R.; Bowman, F.; Collins, D.; Klockow, D.; Flagan, R. C.; Seinfeld, J. H. Formation of Organic Aerosols from the Oxidation of Biogenic Hydrocarbons. *J. Atmos. Chem.* **1997**, *26*, 189–222.
- (15) Johnson, D.; Marston, G. The Gas-Phase Ozonolysis of Unsaturated Volatile Organic Compounds in the Troposphere. *Chem. Soc. Rev.* **2008**, *37*, 699–716.
- (16) Kröll, J. H.; Seinfeld, J. H. Chemistry of Secondary Organic Aerosol: Formation and Evolution of Low-Volatility Organics in the Atmosphere. *Atmos. Environ.* **2008**, *42*, 3593–3624.
- (17) Yu, J.; Cocker, D. R., III; Griffin, R. J.; Flagan, R. C.; Seinfeld, J. H. Gas-Phase Ozone Oxidation of Monoterpenes: Gaseous and Particulate Products. *J. Atmos. Chem.* **1999**, *34*, 207–258.
- (18) Bonn, B.; Moorgat, G. K. New Particle Formation during α - and β -Pinene Oxidation by O₃, OH and NO₃, and the Influence of Water Vapour: Particle Size Distribution Studies. *Atmos. Chem. Phys.* **2002**, *2*, 183–196.
- (19) Spittler, M.; Barnes, I.; Bejan, I.; Brockmann, K. J.; Benter, T.; Wirtz, K. Reactions of NO₃ Radicals with Limonene and α -Pinene: Product and SOA Formation. *Atmos. Environ.* **2006**, *40*, 116–127.
- (20) Perraud, V.; Bruns, E. A.; Ezell, M. J.; Johnson, S. N.; Greaves, J.; Finlayson-Pitts, B. J. Identification of Organic Nitrates in the NO₃ Radical Initiated Oxidation of α -Pinene by Atmospheric Pressure Chemical Ionization Mass Spectrometry. *Environ. Sci. Technol.* **2010**, *44*, 5887–5893.
- (21) Fry, J. L.; Kiendler-Scharr, A.; Rollins, A. W.; Wooldridge, P. J.; Brown, S. S.; Fuchs, H.; Dubé, W.; Mensah, A.; Dal Maso, M.; Tillmann, R. Organic Nitrate and Secondary Organic Aerosol Yield from NO₃ Oxidation of β -Pinene Evaluated Using a Gas-Phase Kinetics/aerosol Partitioning Model. *Atmos. Chem. Phys.* **2009**, *9*, 1431–1449.
- (22) Draper, D. C.; Farmer, D. K.; Desyaterik, Y.; Fry, J. L. A Qualitative Comparison of Secondary Organic Aerosol Yields and Composition from Ozonolysis of Monoterpenes at Varying Concentrations of NO₂. *Atmos. Chem. Phys.* **2015**, *15*, 12267–12281.
- (23) Fry, J. L.; Draper, D. C.; Barsanti, K. C.; Smith, J. N.; Ortega, J.; Winkler, P. M.; Lawler, M. J.; Brown, S. S.; Edwards, P. M.; Cohen, R. C. Secondary Organic Aerosol Formation and Organic Nitrate Yield from NO₃ Oxidation of Biogenic Hydrocarbons. *Environ. Sci. Technol.* **2014**, *48*, 11944–11953.
- (24) Fry, J. L.; Kiendler-Scharr, A.; Rollins, A. W.; Brauers, T.; Brown, S. S.; Dorn, H.-P.; Dubé, W. P.; Fuchs, H.; Mensah, A.; Rohrer, F. SOA from Limonene: Role of NO₃ in Its Generation and Degradation. *Atmos. Chem. Phys.* **2011**, *11*, 3879–3894.
- (25) Jaoui, M.; Kleindienst, T. E.; Docherty, K. S.; Lewandowski, M.; Offenber, J. H. Secondary Organic Aerosol Formation from the Oxidation of a Series of Sesquiterpenes: α -Cedrene, β -Caryophyllene, α -Humulene and α -Farnesene with O₃, OH and NO₃ Radicals. *Environ. Chem.* **2013**, *10*, 178–193.
- (26) Canosa-Mas, C. E.; King, M. D.; Scarr, P. J.; Thompson, K. C.; Wayne, R. P. An Experimental Study of the Gas-Phase Reactions of the NO₃ Radical with Three Sesquiterpenes: Isolongifolene, Alloisolongifolene, and α -Neoclovene. *Phys. Chem. Chem. Phys.* **1999**, *1*, 2929–2933.
- (27) Boyd, C. M.; Sanchez, J.; Xu, L.; Eugene, A. J.; Nah, T.; Tuet, W. Y.; Guzman, M. I.; Ng, N. L. Secondary Organic Aerosol Formation from the β -Pinene + NO₃ System: Effect of Humidity and Peroxy Radical Fate. *Atmos. Chem. Phys.* **2015**, *15*, 7497–7522.
- (28) Nah, T.; Sanchez, J.; Boyd, C. M.; Ng, N. L. Photochemical Aging of α -Pinene and β -Pinene Secondary Organic Aerosol Formed from Nitrate Radical Oxidation. *Environ. Sci. Technol.* **2016**, *50*, 222–231.
- (29) Ayres, B. R.; Allen, H. M.; Draper, D. C.; Brown, S. S.; Wild, R. J.; Jimenez, J. L.; Day, D. A.; Campuzano-Jost, P.; Hu, W.; Gouw, J. de. Organic Nitrate Aerosol Formation via NO₃ + Biogenic Volatile Organic Compounds in the Southeastern United States. *Atmos. Chem. Phys.* **2015**, *15*, 13377–13392.
- (30) Wayne, R. P.; Barnes, I.; Biggs, P.; Burrows, J. P.; Canosa-Mas, C. E.; Hjorth, J.; Le Bras, G.; Moortgat, G. K.; Perner, D.; Poulet, G. The Nitrate Radical: Physics, Chemistry, and the Atmosphere. *Atmos. Environ., Part A* **1991**, *25*, 1–203.
- (31) Sindelarova, K.; Granier, C.; Bouarar, I.; Guenther, A.; Tilmes, S.; Stavrou, T.; Müller, J.-F.; Kuhn, U.; Stefani, P.; Knorr, W. Global Data Set of Biogenic VOC Emissions Calculated by the MEGAN Model over the Last 30 Years. *Atmos. Chem. Phys.* **2014**, *14*, 9317–9341.
- (32) Atkinson, R.; Arey, J. Atmospheric Degradation of Volatile Organic Compounds. *Chem. Rev.* **2003**, *103*, 4605–4638.
- (33) Shu, Y.; Atkinson, R. Rate Constants for the Gas-phase Reactions of O₃ with a Series of Terpenes and OH Radical Formation from the O₃ Reactions with Sesquiterpenes at 296 ± 2 K. *Int. J. Chem. Kinet.* **1994**, *26*, 1193–1205.

- (34) Shu, Y.; Atkinson, R. Atmospheric Lifetimes and Fates of a Series of Sesquiterpenes. *J. Geophys. Res.* **1995**, *100*, 7275–7281.
- (35) Griffin, R. J.; Cocker, D. R.; Flagan, R. C.; Seinfeld, J. H. Organic Aerosol Formation from the Oxidation of Biogenic Hydrocarbons. *J. Geophys. Res.* **1999**, *104*, 3555–3567.
- (36) Shiraiwa, M.; Berkemeier, T.; Schilling-Fahnestock, K. A.; Seinfeld, J. H.; Pöschl, U. Molecular Corridors and Kinetic Regimes in the Multiphase Chemical Evolution of Secondary Organic Aerosol. *Atmos. Chem. Phys.* **2014**, *14*, 8323–8341.
- (37) Li, Y.; Pöschl, U.; Shiraiwa, M. Molecular Corridors and Parameterizations of Volatility in the Chemical Evolution of Organic Aerosols. *Atmos. Chem. Phys.* **2016**, *16*, 3327–3344.
- (38) Nguyen, T. B.; Bateman, A. P.; Bones, D. L.; Nizkorodov, S. A.; Laskin, J.; Laskin, A. High-Resolution Mass Spectrometry Analysis of Secondary Organic Aerosol Generated by Ozonolysis of Isoprene. *Atmos. Environ.* **2010**, *44*, 1032–1042.
- (39) Kourtchev, I.; Giorio, C.; Manninen, A.; Wilson, E.; Mahon, B.; Aalto, J.; Kajos, M.; Venables, D.; Ruuskanen, T.; Levula, J. Enhanced Volatile Organic Compounds Emissions and Organic Aerosol Mass Increase the Oligomer Content of Atmospheric Aerosols. *Sci. Rep.* **2016**, *6*, 35038.
- (40) Lignell, H.; Epstein, S. A.; Marvin, M. R.; Shemesh, D.; Gerber, B.; Nizkorodov, S. Experimental and Theoretical Study of Aqueous Cis-Pinonic Acid Photolysis. *J. Phys. Chem. A* **2013**, *117*, 12930–12945.
- (41) Madronich, S. *Tropospheric Ultraviolet and Visible (TUV) Radiation Model*. <http://cprm.acd.ucar.edu/Models/TUV/index.shtml> (accessed May 2016).
- (42) Bateman, A. P.; Laskin, J.; Laskin, A.; Nizkorodov, S. A. Applications of High-Resolution Electrospray Ionization Mass Spectrometry to Measurements of Average Oxygen to Carbon Ratios in Secondary Organic Aerosols. *Environ. Sci. Technol.* **2012**, *46*, 8315–8324.
- (43) Bateman, A. P.; Nizkorodov, S. A.; Laskin, J.; Laskin, A. Time-Resolved Molecular Characterization of Limonene/ozone Aerosol Using High-Resolution Electrospray Ionization Mass Spectrometry. *Phys. Chem. Chem. Phys.* **2009**, *11*, 7931–7942.
- (44) Nguyen, T. B.; Roach, P. J.; Laskin, J.; Laskin, A.; Nizkorodov, S. A. Effect of Humidity on the Composition of Isoprene Photooxidation Secondary Organic Aerosol. *Atmos. Chem. Phys.* **2011**, *11*, 6931–6944.
- (45) Nguyen, T. B.; Laskin, J.; Laskin, A.; Nizkorodov, S. A. Nitrogen-Containing Organic Compounds and Oligomers in Secondary Organic Aerosol Formed by Photooxidation of Isoprene. *Environ. Sci. Technol.* **2011**, *45*, 6908–6918.
- (46) Kind, T.; Fiehn, O. Seven Golden Rules for Heuristic Filtering of Molecular Formulas Obtained by Accurate Mass Spectrometry. *BMC Bioinf.* **2007**, *8*, 1.
- (47) Pankow, J. F. An Absorption-Model of Gas-Particle Partitioning of Organic-Compounds in the Atmosphere. *Atmos. Environ.* **1994**, *28*, 185–188.
- (48) Pankow, J. F. An Absorption-Model of the Gas Aerosol Partitioning Involved in the Formation of Secondary Organic Aerosol. *Atmos. Environ.* **1994**, *28*, 189–193.
- (49) Donahue, N. M.; Robinson, A. L.; Stanier, C. O.; Pandis, S. N. Coupled Partitioning, Dilution, and Chemical Aging of Semivolatile Organics. *Environ. Sci. Technol.* **2006**, *40*, 2635–2643.
- (50) Cech, N. B.; Enke, C. G. Practical Implications of Some Recent Studies in Electrospray Ionization Fundamentals. *Mass Spectrom. Rev.* **2001**, *20*, 362–387.
- (51) Nguyen, T. B.; Nizkorodov, S. A.; Laskin, A.; Laskin, J. An Approach toward Quantification of Organic Compounds in Complex Environmental Samples Using High-Resolution Electrospray Ionization Mass Spectrometry. *Anal. Methods* **2013**, *5*, 72–80.
- (52) Wängberg, I.; Barnes, I.; Becker, K. H. Product and Mechanistic Study of the Reaction of NO₃ Radicals with α -Pinene. *Environ. Sci. Technol.* **1997**, *31*, 2130–2135.
- (53) Heaton, K. J.; Dreyfus, M. A.; Wang, S.; Johnston, M. V. Oligomers in the Early Stage of Biogenic Secondary Organic Aerosol Formation and Growth. *Environ. Sci. Technol.* **2007**, *41*, 6129–6136.
- (54) Baltensperger, U.; Kalberer, M.; Dommen, J.; Paulsen, D.; Alfarra, M. R.; Coe, H.; Fisseha, R.; Gascho, A.; Gysel, M.; Nyeki, S.; et al. Secondary Organic Aerosols from Anthropogenic and Biogenic Precursors. *Faraday Discuss.* **2005**, *130*, 265–278.
- (55) Reinhardt, A.; Emmenegger, C.; Gerrits, B.; Panse, C.; Dommen, J.; Baltensperger, U.; Zenobi, R.; Kalberer, M. Ultrahigh Mass Resolution and Accurate Mass Measurements as a Tool to Characterize Oligomers in Secondary Organic Aerosols. *Anal. Chem.* **2007**, *79*, 4074–4082.
- (56) Tolocka, M. P.; Jang, M.; Ginter, J. M.; Cox, F. J.; Kamens, R. M.; Johnston, M. V. Formation of Oligomers in Secondary Organic Aerosol. *Environ. Sci. Technol.* **2004**, *38*, 1428–1434.
- (57) Gao, Y. Q.; Hall, W. A.; Johnston, M. V. Molecular Composition of Monoterpene Secondary Organic Aerosol at Low Mass Loading. *Environ. Sci. Technol.* **2010**, *44*, 7897–7902.
- (58) Glasius, M.; Duane, M.; Larsen, B. R. Determination of Polar Terpene Oxidation Products in Aerosols by Liquid Chromatography-Ion Trap Mass Spectrometry. *J. Chromatogr. A* **1999**, *833*, 121–135.
- (59) Kahnt, A.; Iinuma, Y.; Mutzel, A.; Böge, O.; Claeys, M.; Herrmann, H. Campholenic Aldehyde Ozonolysis: A Mechanism Leading to Specific Biogenic Secondary Organic Aerosol Constituents. *Atmos. Chem. Phys.* **2014**, *14*, 719–736.
- (60) Winterhalter, R.; Dingenen, R.; Van Larsen, B. R.; Jensen, N. R.; Hjorth, J. LC-MS Analysis of Aerosol Particles from the Oxidation of α -Pinene by Ozone and OH-Radicals. *Atmos. Chem. Phys. Discuss.* **2003**, *3*, 1–39.
- (61) Iinuma, Y.; Böge, O.; Miao, Y.; Sierau, B.; Gnauk, T.; Herrmann, H. Laboratory Studies on Secondary Organic Aerosol Formation from Terpenes. *Faraday Discuss.* **2005**, *130*, 279–294.
- (62) Venkatachari, P.; Hopke, P. K. Characterization of Products Formed in the Reaction of Ozone with α -Pinene: Case for Organic Peroxides. *J. Environ. Monit.* **2008**, *10*, 966–974.
- (63) Camredon, M.; Hamilton, J. F.; Alam, M. S.; Wyche, K. P.; Carr, T.; White, I. R.; Monks, P. S.; Rickard, A. R.; Bloss, W. J. Distribution of Gaseous and Particulate Organic Composition during Dark α -Pinene Ozonolysis. *Atmos. Chem. Phys.* **2010**, *10*, 2893–2917.
- (64) Putman, A. L.; Offenber, J. H.; Fisseha, R.; Kundu, S.; Rahn, T. A.; Mazzoleni, L. R. Ultrahigh-Resolution FT-ICR Mass Spectrometry Characterization of α -Pinene Ozonolysis SOA. *Atmos. Environ.* **2012**, *46*, 164–172.
- (65) Müller, L.; Reinnig, M.; Hayen, H.; Hoffmann, T. Characterization of Oligomeric Compounds in Secondary Organic Aerosol Using Liquid Chromatography Coupled to Electrospray Ionization Fourier Transform Ion Cyclotron Resonance Mass Spectrometry. *Rapid Commun. Mass Spectrom.* **2009**, *23*, 971–979.
- (66) Kristensen, K.; Watne, Å. K.; Hammes, J.; Lutz, A.; Petäjä, T.; Hallquist, M.; Bilde, M.; Glasius, M. High-Molecular Weight Dimer Esters Are Major Products in Aerosols from α -Pinene Ozonolysis and the Boreal Forest. *Environ. Sci. Technol. Lett.* **2016**, *3*, 280–285.
- (67) Beck, M.; Hoffmann, T. A Detailed MS^N Study for the Molecular Identification of a Dimer Formed from Oxidation of Pinene. *Atmos. Environ.* **2016**, *130*, 120–126.
- (68) Kristensen, K.; Cui, T.; Zhang, H.; Gold, A.; Glasius, M.; Surratt, J. D. Dimers in α -Pinene Secondary Organic Aerosol: Effect of Hydroxyl Radical, Ozone, Relative Humidity and Aerosol Acidity. *Atmos. Chem. Phys.* **2014**, *14*, 4201–4218.
- (69) Yasmeen, F.; Vermeylen, R.; Szmigielski, R.; Iinuma, Y.; Böge, O.; Herrmann, H.; Maenhaut, W.; Claeys, M. Terpenylic Acid and Related Compounds: Precursors for Dimers in Secondary Organic Aerosol from the Ozonolysis of α - and β -Pinene. *Atmos. Chem. Phys.* **2010**, *10*, 9383–9392.
- (70) Noziere, B.; Kalberer, M.; Claeys, M.; Allan, J.; D'Anna, B.; Decesari, S.; Finessi, E.; Glasius, M.; Grgic, I.; Hamilton, J. F.; et al. The Molecular Identification of Organic Compounds in the Atmosphere: State of the Art and Challenges. *Chem. Rev.* **2015**, *115*, 3919–3983.
- (71) Beck, M.; Winterhalter, R.; Herrmann, F.; Moortgat, G. K. The Gas-Phase Ozonolysis of α -Humulene. *Phys. Chem. Chem. Phys.* **2011**, *13*, 10970–11001.

- (72) Jaoui, M.; Kamens, R. M. Gas and Particulate Products Distribution from the Photooxidation of α -Humulene in the Presence of NO_x, Natural Atmospheric Air and Sunlight. *J. Atmos. Chem.* **2003**, *46*, 29–54.
- (73) Ng, N. L.; Kroll, J. H.; Keywood, M. D.; Bahreini, R.; Varutbangkul, V.; Flagan, R. C.; Seinfeld, J. H.; Lee, A.; Goldstein, A. H. Contribution of First- versus Second-Generation Products to Secondary Organic Aerosols Formed in the Oxidation of Biogenic Hydrocarbons. *Environ. Sci. Technol.* **2006**, *40*, 2283–2297.
- (74) Aiken, A. C.; Decarlo, P. F.; Kroll, J. H.; Worsnop, D. R.; Huffman, J. A.; Docherty, K. S.; Ulbrich, I. M.; Mohr, C.; Kimmel, J. R.; Sueper, D.; et al. O/C and OM/OC Ratios of Primary, Secondary, and Ambient Organic Aerosols with High-Resolution Time-of-Flight Aerosol Mass Spectrometry. *Environ. Sci. Technol.* **2008**, *42*, 4478–4485.
- (75) Brinkmann, T.; Horsch, P.; Sartorius, D.; Frimmel, F. H. Photoformation of Low-Molecular-Weight Organic Acids from Brown Water Dissolved Organic Matter. *Environ. Sci. Technol.* **2003**, *37*, 4190–4198.
- (76) Kujawinski, E. B.; Del Vecchio, R.; Blough, N. V.; Klein, G. C.; Marshall, A. G. Probing Molecular-Level Transformations of Dissolved Organic Matter: Insights on Photochemical Degradation and Protozoan Modification of DOM from Electrospray Ionization Fourier Transform Ion Cyclotron Resonance Mass Spectrometry. *Mar. Chem.* **2004**, *92*, 23–37.
- (77) Romonosky, D. E.; Nguyen, L. Q.; Shemesh, D.; Nguyen, T. B.; Epstein, S. A.; Martin, D. B. C.; Vanderwal, C. D.; Gerber, R. B.; Nizkorodov, S. A. Absorption Spectra and Aqueous Photochemistry of β -Hydroxyalkyl Nitrates of Atmospheric Interest. *Mol. Phys.* **2015**, *113*, 2179–2190.
- (78) Müller, J.-F.; Peeters, J.; Stavrou, T. Fast Photolysis of Carbonyl Nitrates from Isoprene. *Atmos. Chem. Phys.* **2014**, *14*, 2497–2508.
- (79) Darer, A. I.; Cole-Filipiak, N. C.; O'Connor, A. E.; Elrod, M. J. Formation and Stability of Atmospherically Relevant Isoprene-Derived Organosulfates and Organonitrates. *Environ. Sci. Technol.* **2011**, *45*, 1895–1902.
- (80) Hu, K. S.; Darer, A. I.; Elrod, M. J. Thermodynamics and Kinetics of the Hydrolysis of Atmospherically Relevant Organonitrates and Organosulfates. *Atmos. Chem. Phys.* **2011**, *11*, 8307–8320.
- (81) Liu, S.; Shilling, J. E.; Song, C.; Hiranuma, N.; Zaveri, R. A.; Russell, L. M. Hydrolysis of Organonitrate Functional Groups in Aerosol Particles. *Aerosol Sci. Technol.* **2012**, *46*, 1359–1369.
- (82) Badali, K. M.; Zhou, S.; Aljawhary, D.; Antiñolo, M.; Chen, W. J.; Lok, A.; Mungall, E.; Wong, J. P. S.; Zhao, R.; Abbatt, J. P. D. Formation of Hydroxyl Radicals from Photolysis of Secondary Organic Aerosol Material. *Atmos. Chem. Phys.* **2015**, *15*, 7831–7840.
- (83) Tong, H.; Arangio, A. M.; Lakey, P. S. J.; Berkemeier, T.; Liu, F.; Kampf, C. J.; Brune, W. H.; Pöschl, U.; Shiraiwa, M. Hydroxyl Radicals from Secondary Organic Aerosol Decomposition in Water. *Atmos. Chem. Phys.* **2016**, *16*, 1761–1771.
- (84) Aljawhary, D.; Zhao, R.; Lee, A. K. Y.; Wang, C.; Abbatt, J. P. D. Kinetics, Mechanism, and Secondary Organic Aerosol Yield of Aqueous Phase Photo-Oxidation of α -Pinene Oxidation Products. *J. Phys. Chem. A* **2016**, *120*, 1395–1407.
- (85) Chacon-Madrid, H. J.; Donahue, N. M. Fragmentation vs. Functionalization: Chemical Aging and Organic Aerosol Formation. *Atmos. Chem. Phys.* **2011**, *11*, 10553–10563.
- (86) Kroll, J. H.; Smith, J. D.; Che, D. L.; Kessler, S. H.; Worsnop, D. R.; Wilson, K. R. Measurement of Fragmentation and Functionalization Pathways in the Heterogeneous Oxidation of Oxidized Organic Aerosol. *Phys. Chem. Chem. Phys.* **2009**, *11*, 8005–8014.
- (87) Lambe, A. T.; Onasch, T. B.; Croasdale, D. R.; Wright, J. P.; Martin, A. T.; Franklin, J. P.; Massoli, P.; Kroll, J. H.; Canagaratna, M. R.; Brune, W. H. Transitions from Functionalization to Fragmentation Reactions of Laboratory Secondary Organic Aerosol (SOA) Generated from the OH Oxidation of Alkane Precursors. *Environ. Sci. Technol.* **2012**, *46*, 5430–5437.
- (88) Perraud, V.; Bruns, E. A.; Ezell, M. J.; Johnson, S. N.; Yu, Y.; Alexander, M. L.; Zelenyuk, A.; Imre, D.; Chang, W. L.; Dabdub, D. Nonequilibrium Atmospheric Secondary Organic Aerosol Formation and Growth. *Proc. Natl. Acad. Sci. U. S. A.* **2012**, *109*, 2836–2841.
- (89) Lee, B. H.; Mohr, C.; Lopez-Hilfiker, F. D.; Lutz, A.; Hallquist, M.; Lee, L.; Romer, P.; Cohen, R. C.; Iyer, S.; Kurtén, T. Highly Functionalized Organic Nitrates in the Southeast United States: Contribution to Secondary Organic Aerosol and Reactive Nitrogen Budgets. *Proc. Natl. Acad. Sci. U. S. A.* **2016**, *113*, 1516–1521.
- (90) Malecha, K. T.; Nizkorodov, S. A. Photodegradation of Secondary Organic Aerosol Particles as a Source of Small, Oxygenated Volatile Organic Compounds. *Environ. Sci. Technol.* **2016**, *50*, 9990–9997.
- (91) Lignell, H.; Hinks, M. L.; Nizkorodov, S. A. Exploring Matrix Effects on Photochemistry of Organic Aerosols. *Proc. Natl. Acad. Sci. U. S. A.* **2014**, *111*, 13780–13785.
- (92) Hinks, M. L.; Brady, M. V.; Lignell, H.; Song, M.; Grayson, J. W.; Bertram, A. K.; Lin, P.; Laskin, A.; Laskin, J.; Nizkorodov, S. A. Effect of Viscosity on Photodegradation Rates in Complex Secondary Organic Aerosol Materials. *Phys. Chem. Chem. Phys.* **2016**, *18*, 8785–8793.
- (93) Lee, A. K. Y.; Zhao, R.; Gao, S. S.; Abbatt, J. P. D. Aqueous-Phase OH Oxidation of Glyoxal: Application of a Novel Analytical Approach Employing Aerosol Mass Spectrometry and Complementary off-Line Techniques. *J. Phys. Chem. A* **2011**, *115*, 10517–10526.
- (94) Tan, Y.; Carlton, A. G.; Seitzinger, S. P.; Turpin, B. J. SOA from Methylglyoxal in Clouds and Wet Aerosols: Measurement and Prediction of Key Products. *Atmos. Environ.* **2010**, *44*, 5218–5226.
- (95) Waxman, E. M.; Dzepina, K.; Ervens, B.; Lee-Taylor, J.; Aumont, B.; Jimenez, J. L.; Madronich, S.; Volkamer, R. Secondary Organic Aerosol Formation from Semi- and Intermediate-Volatility Organic Compounds and Glyoxal: Relevance of O/C as a Tracer for Aqueous Multiphase Chemistry. *Geophys. Res. Lett.* **2013**, *40*, 978–982.